Refraction of cylindrical converging shock wave at an air/helium gaseous interface

Zhigang Zhai, Wei Li, Ting Si, Xisheng Luo, Jiming Yang, and Xiyun Lu

Citation: Phys. Fluids **29**, 016102 (2017); doi: 10.1063/1.4973825
View online: http://dx.doi.org/10.1063/1.4973825
View Table of Contents: http://aip.scitation.org/toc/phf/29/1
Published by the American Institute of Physics

Refraction of cylindrical converging shock wave at an air/helium gaseous interface

Zhigang Zhai,[a] Wei Li, Ting Si, Xisheng Luo, Jiming Yang, and Xiyun Lu
Advanced Propulsion Laboratory, Department of Modern Mechanics, University of Science and Technology of China, Hefei 230026, China

(Received 22 August 2016; accepted 27 December 2016; published online 18 January 2017)

Refraction of a cylindrical converging shock wave at an inclined air/helium interface is investigated. Experimentally, based on the shock dynamics theory, a special wall profile is designed to generate a perfectly cylindrical converging shock wave. A soap film technique is developed to form an inclined discontinuous air/helium interface, and high-speed schlieren photography is adopted to capture the flow. Numerical simulations are also performed to compare with the experimental counterparts and to show details of refraction. In this work, two initial incident angles (45° and 60°) are considered. As the incident shock converges inward, the shock intensity increases while the incident angle decreases, causing possible transitions among the wave patterns. For the case of 45°, an irregular refraction of free precursor refraction (FPR) first occurs and gradually transits into regular refraction, while for the case of 60°, various irregular refractions of twin von Neumann refraction (TNR), twin regular refraction (TRR), free precursor von Neumann refraction (FNR), and FPR occur in sequence. The transition sequences do not belong to any groups described in the planar counterpart, indicating that the classification of the refraction phenomenon in the planar case is not exhaustive or cannot be applied to the converging case. It is also the first time to observe the transition from FNR to FPR, providing an experimental evidence for the previous numerical results. It is deemed that the difference between the velocities of the incident and transmitted shocks propagating along the interface is the primary factor that induces the transitions among wave patterns. *Published by AIP Publishing.* [http://dx.doi.org/10.1063/1.4973825]

I. INTRODUCTION

When a planar shock wave passes across a gaseous interface inhomogeneity, wave refraction and reflection take place accompanied by interface deformation as the acoustic impedance changes. In recent years, with the studies of the shock-induced mixing for scramjet combustors[1] and inertial confinement fusion,[2] the interference of the shock waves with a mixed gas of fuels and the interaction of the shock waves with density inhomogeneities have gained extensive attention as one of the topics of turbulent mixing. This environment has been referred to as the shock-induced Richtmyer-Meshkov (RM) instability.[3,4] Understanding the formation of wave pattern and its effects on interface evolution has long been an important subject of research. Because the phenomena of the wave refractions at a gaseous interface are very complicated, especially for irregular refractions, it is difficult to obtain the analytical solutions. Therefore, previous researchers mainly studied simplified models. Taub[5] and Polachek and Seeger[6] independently formulated the theoretical description of a planar shock wave refracting at a tilted interface between gases with different sound speeds at first. Then the shock wave refraction theory was further extended via various ways.[7–11] The earliest experiment was carried out by Jahn,[12] who studied the refraction of a planar shock wave at a tilted gaseous interface between air/CO_2 and air/CH_4. Subsequently, a systematically experimental investigation on a planar shock refracting at a tilted gaseous interface was performed,[13–15] and various irregular refraction phenomena were observed and discussed. In their studies, the shock refractions were separated into two major groups: "slow/fast" and "fast/slow" based on the difference in acoustic impedances of two gases across the interface. In terms of incident shock intensity, the types of refraction within the slow/fast group were further subdivided into three classes: very weak, weak, and strong.[15] Besides, the numerical simulations on refraction of a planar shock wave at a tilted gaseous interface were also extensively performed,[16–19] and comparison with the experimental results was made. According to these studies, three factors, including the incident shock intensity, incident angle (defined as the angle of the incident shock front with the interface), and the acoustic impedances of gases on both sides of interface, will affect the shock refraction type.

Most previous studies concentrated on a planar shock wave refracting at a tilted gaseous interface, in which both the shock strength and the incident angle are constants. Thus, the phenomenon and laws obtained from these studies were limited to steady or quasi-steady conditions. Phenomena of a planar shock wave refracting at a non-planar interface are more complicated,[20–22] in which the shock strength is fixed while the incident angle varies continuously. However, in most practical applications, such as underwater explosion and spherical converging shock wave interaction with a capsule in inertial

[a]Electronic mail: sanjing@ustc.edu.cn

confinement fusion, the shock wave is curved and the flow behind the curved shock is unsteady. As we know, shock intensity and incident angle are the two most important factors that affect the wave patterns of refraction. When a converging shock wave refracts at a tilted gaseous interface, the converging shock intensity and incident angle change continuously with the shock wave moving forward. Therefore, the refraction phenomena and laws in unsteady condition are not necessarily the same as those obtained from steady or quasi-steady conditions completely. It is therefore of fundamental interest and practical significance to explore the fluid dynamics of the flows when a converging shock wave refracts at a tilted gaseous interface. Due to the difficulties encountered in generating a converging shock wave, the refraction of a converging shock wave at a gaseous interface was rarely studied before. Previously, several methods[23–25] were proposed to generate a converging shock wave in a shock tube. In our previous work,[26] a cylindrical converging shock wave was generated based on the shock dynamics theory, providing an essential prerequisite for the investigation of a converging shock wave refracting at an interface.

An initial inclined interface is another crucial factor for investigating the shock refraction phenomena in experiment. In previous work, a delicate polymer membrane with the thickness of about ten molecules was adopted to separate one gas from another,[13,15] and the shock refraction phenomena were investigated. Organic films[27] and nitrocellulose membrane with a support[28] were also adopted to form an inclined interface, focusing on the RM instability of the inclined interface. Recently, an inclined diffusive interface was generated by McFarland *et al.* in their inclined shock tube[29–31] to investigate the RM instability of the inclined interface using laser sheet technique. However, such a diffusive interface is inadequate to investigate the shock refraction phenomenon. In our group, the soap film technique was extended to form a discontinuous "V" shaped interface,[32,33] and interface evolution after shock acceleration was investigated with little attention to the shock refraction phenomenon. Unfortunately, such an interface formation method cannot be directly applied to the converging test section. In this work, in order to investigate the refraction of a cylindrical converging shock wave at an inclined gaseous interface, a new soap film technique is developed to form an inclined gaseous interface separating one gas from another.

II. EXPERIMENTAL AND NUMERICAL METHODS

A. Experimental method

A specially designed converging shock tube is manufactured according to our previous work,[26,34] which can convert a planar incident shock wave into a cylindrical converging one. The converging shock tube consists of a 2 m long driver section, a 4 m long driven section with cross sectional area of 95 mm × 95 mm, and a 1 m long transition section with cross sectional area of 300 mm × 30 mm, and a 1 m long converging test section. The variation of cross sectional area is for the generation of soap film interface easily. In the current experiment, the converging angle θ_0 is 25° and the initial shock wave in planar section has a Mach number of $M_0 = 1.4$. Under these conditions, the radius of the converging section is 208.5 mm, and the shock Mach number increases to 1.58 at the beginning of the converging section. As indicated in Fig. 1(a), the incident angle ω_i is defined as the angle between the interface and the tangent of intersection of the cylindrical shock wave with the interface. Note that the incident angle varies along the shock front because of the shock curvature effect for the cylindrical case, which is completely different from the planar shock case where only one invariant incident angle exists. For the current study, the variation range of the incident angle is about 25° during the converging shock wave moving along the interface if a perfectly cylindrical shape of the shock is assumed, i.e., the shock shape and shock strength will not be disturbed by the interface. It should be mentioned here that the position of the initial gaseous interface determines the incident angle and the intensity of the incident cylindrical shock wave when it arrives at the interface, i.e., the two most important factors that influence the wave refraction patterns, will both change with the variation of the initial interface position. As a consequence, different wave refraction phenomena may occur if the incident shock wave at different positions collides with the gaseous interface. Actually, the position of the initial interface in the present experiments is arbitrary provided that the interface locates within the converging region. In this work, in order to form the initial gaseous interface easily, the position of the leading edge of the interface for two cases is fixed as 13.5 mm away from the start of the converging section, i.e., R = 195 mm. When the converging shock wave meets the interface, its intensity increases to 1.60.

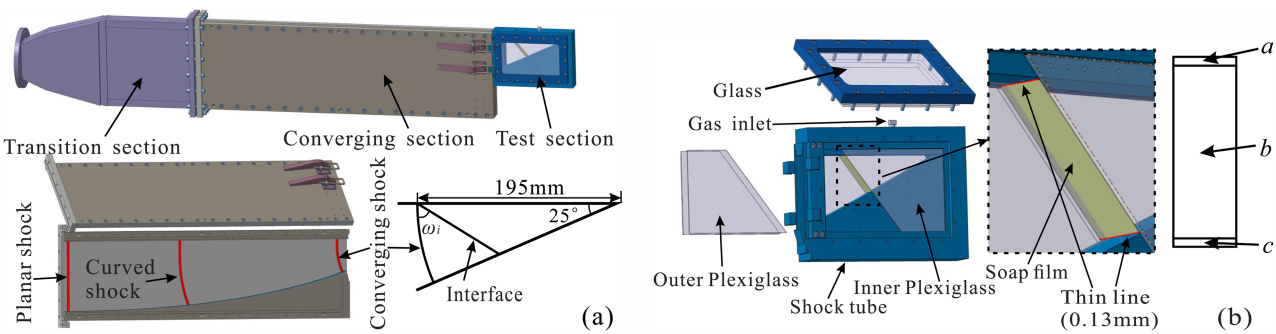

FIG. 1. Schematics of the shock tube (a), the test section and gaseous interface (b).

Soap film is an excellent gaseous interface material for shock-interface experiment because of its durability and limited thickness. It is so thin (about 0.25–1 μm)[35] that it has very little effect on the experimental results. In this work, the extended soap film technique similar to our previous work[36] is adopted to create a discontinuous inclined interface. As shown in Fig. 1(b), two inner Plexiglases (with a thickness of 3 mm) with an oblique angle are first fixed on both sides of the test section by a sealant, forming a cavity of triangular prism shape with one face opening to be covered with soap film. Due to the surface tension, the soap film cannot contact the sidewall of the test section directly. Therefore, two thin lines with a diameter of 0.13 mm are stuck on the Plexiglases to separate the soap film interface into three parts (*a*, *b*, and *c*). Part *b* will keep the designed angle with the sidewall, while parts *a* and *c* will move along the sidewall slightly until they reach a balance. The gap between the thin line and the sidewall can be controlled to be smaller than 1 mm so that parts *a* and *c* are narrow enough to have limited effect on the wave pattern. In order to form an air/helium interface, in the experiment, parts *a* and *b* will be formed first, while part *c* will be left open as a gas outlet. Helium is pumped into the cavity through the gas inlet, and air in the cavity will be squeezed out through part *c* because helium is lighter than air. Meanwhile, two needles connected to an air extractor will also be threaded into the cavity to accelerate the process of exhaust. An oxygen detector located at part *c* is used to monitor the purity of helium in the cavity. The measuring range of the oxygen detector is 0%–25% VOL, and the accuracy is 0.1% VOL. In our experiments, when the concentration of oxygen in air is lower than 0.5% VOL, it is considered that the air in the cavity has been replaced by helium completely. Once the concentration of helium meets the requirement, part *c* will be covered with soap film and gas inlet will be shut down. Afterwards, the outer Plexiglases and the optical glasses will be mounted, and the experiment can be carried out. In this experiment, the angle between the soap film and the sidewall of the test section can be easily changed by replacing the inner and outer Plexiglases to obtain transitions among different wave patterns.

A Z-fold schlieren system made up of a knife-edge, a slit, two convex lenses, two concave mirrors, a LED regulated light source (CEL-HXF300), and a high-speed video camera (FASTCAM SA5, Photron Limited) is adopted, as shown in Fig. 2, to record the evolution of wave patterns. The timing and triggering system involves a four channel delay generator (DG645, Stanford Research Systems), two piezoelectric pressure transducers, a charge amplifier, an oscilloscope, and some accessories. In this work, two different initial incident angles of 45° and 60° are adopted, and the corresponding frame rates of the camera are 140 000 fps and 105 000 fps, respectively. The image sizes are 192 pixel × 192 pixel and 192 pixel × 184 pixel, respectively, and the shutter speed of the camera is 1/2 710 000 s.

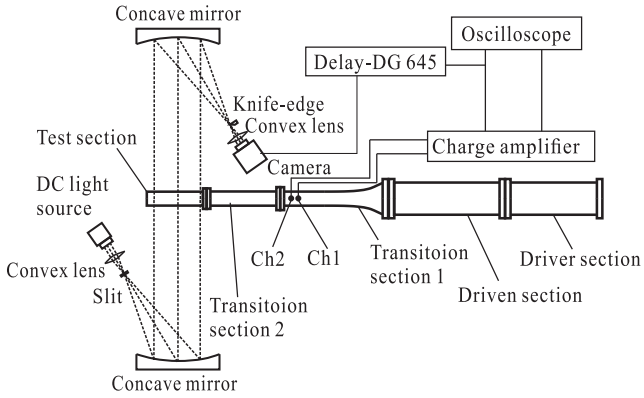

FIG. 2. Schematic of the high speed schlieren photography.

B. Numerical method

An upwind space-time CE/SE (conservation element and solution element) method[37,38] is adopted to simulate the process of a cylindrical converging shock wave refracting at an air/helium interface. This method has been well validated in capturing shocks and details of complex flow structures.[37–39] The details of the method are therefore neglected and only a brief description is provided here. In this method, the numerical flux through the interface of two different conservation elements is determined by an upwind procedure. The upwind procedure breaks the space-time inversion invariance so that it can be directly applied to capture discontinuities without spurious oscillations compared with the original centered CE/SE method. The rotated HLLC (Harten, Lax, van Leer, Contact) Riemann solver is adopted to extend the upwind CE/SE method to two-dimensional simulation. Comparing with the other approximate Riemann solvers (e.g., HLL, Roe), the rotated HLLC introduces the least numerical mixing. The scheme has a second order accuracy in both temporal and spatial scales and employs two-dimensional rectangular meshes. The computational domain is 220 mm × 110 mm and 2000 × 1000 mesh grids are used in the simulations. As sketched in Fig. 1(a), the inflow condition is applied at the left boundary and the reflective condition is imposed on the upper and the lower inclined boundaries. The reflective condition at the lower inclined boundary is generated by extrapolating the variables of each grid inside the boundary to the corresponding grid outside by coordinate transformation. Thus, the normal velocity of the flow on the lower inclined boundary is zero and the tangential velocity is continuous. Then the incident shock is set as a regular circle with the intersection of the upper and the lower inclined boundaries as its focal point. The flow state behind the incident cylindrical shock wave is set to be uniform with velocity radially pointing to the focal point. Actually, the lower inclined boundary is serrated since two dimensional rectangular meshes are adopted. However, because the fine mesh size, i.e., 0.11 mm, is adopted and we do not care about the wave patterns near the boundary, the serrated boundary will have limited influence on the present numerical simulations.

TABLE I. Physical properties of pure gases at T_0 = 293 K and p_0 = 101 325 Pa.

Gas	Molecular weight (g/mol)	Density (kg/m^3)	Sound speed (m/s)	Specific heat ratio
Air	28.967	1.204	343.1	1.4
Helium	4	0.1663	1008	1.667

TABLE II. Physical properties of actual test gas in the numerical simulations at $T_0 = 293$ K and $p_0 = 101\,325$ Pa. m% A + n% B denotes that the gas used is a mixture of m% A and n% B (the mole fraction). For both cases, the incident gas (air) is considered as pure.

Case	Test gas	Molecular weight (g/mol)	Density (kg/m^3)	Sound speed (m/s)	Specific heat ratio
45	85.5% helium + 14.5% air	7.63	0.315	716.5	1.608
60	85% helium + 15% air	7.74	0.320	710.9	1.606

The initial temperature T_0 of 293 K and the initial pressure p_0 of 101 325 Pa are adopted and the physical properties of the pure gases are given in Table I. Because of the gas penetration through the soap film, it is nearly impossible to obtain the pure gases on both sides of the interface, which means that the gas contamination must be considered in experiments. In the experiments, the incident gas (air) is considered as pure due to the huge volume and large density. However, the contamination of helium by air in a cavity cannot be ignored. In order to obtain the actual gas concentration in cavity, the velocities of shocks at both sides of the interface are first experimentally measured from the schlieren pictures and then one-dimensional gas dynamics theory is used to solve the problem of a planar shock wave impinging on a planar or an inclined gaseous interface for each case. Thus the gas concentration in a cavity can be approximately calculated. By adjusting the gas concentration gently, several numerical simulations with different gas concentrations are conducted to compare with the experimental results till the velocities of shocks in numerical simulation match well with the experimental ones. The physical properties of the actual test gas used for each case in the present simulations are listed in Table II.

III. RESULTS AND DISCUSSION

Figure 3 presents the experimental and numerical schlieren images of a cylindrical converging shock wave refracting at an air/helium interface with an initial incident angle $\omega_i = 45°$. The incident shock travels from left to right and the moment when the incident shock collides with the interface is defined as the initial time, i.e., $t = 0$ μs. It can be seen from Fig. 3 that the wave patterns and interface deformation in experiments are quite consistent with numerical counterparts. Differently, the numerical schlieren images are sharper than the experimental ones. In experiment, the interface is formed by soap films which will break up after shock impact. Due to the larger density of soap droplets, its movement is delayed compared with the air/helium interface, resulting in the experimental schlieren images being thicker. At an early stage, we can find that the transmitted shock t moves faster than the incident shock i along the interface (13.98-49.59 μs). In order to show the details of the refraction pattern, the wave pattern at $t = 49.59$ μs is zoomed in and presented in Fig. 4(a). The transmitted shock t moves as a free precursor shock and refracts from helium back into air, forming a shock j in air. The shock j and the incident shock i eventually encounter, and mutually

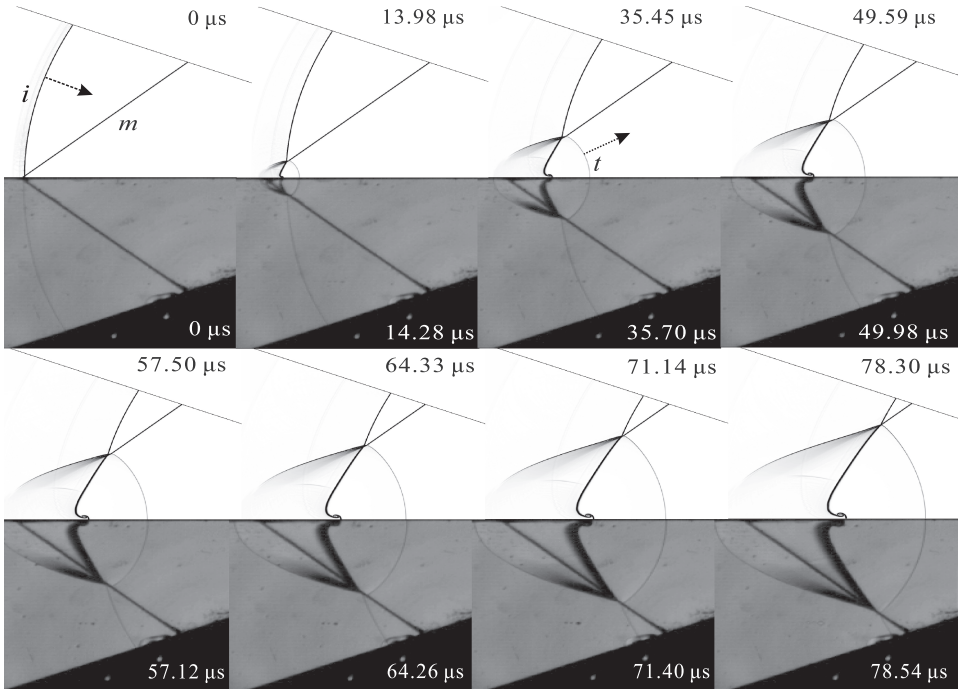

FIG. 3. Sequences of experimental and numerical schlieren frames showing the evolution of a converging shock wave refracting at a tilted interface with an initial incident angle $\omega_i = 45°$. Numbers in the figure indicate the time of the shock impact (similarly hereinafter). i, incident shock; t, transmitted shock; m, undisturbed material interface. The dashed arrows indicate the shock moving directions and similarly hereinafter.

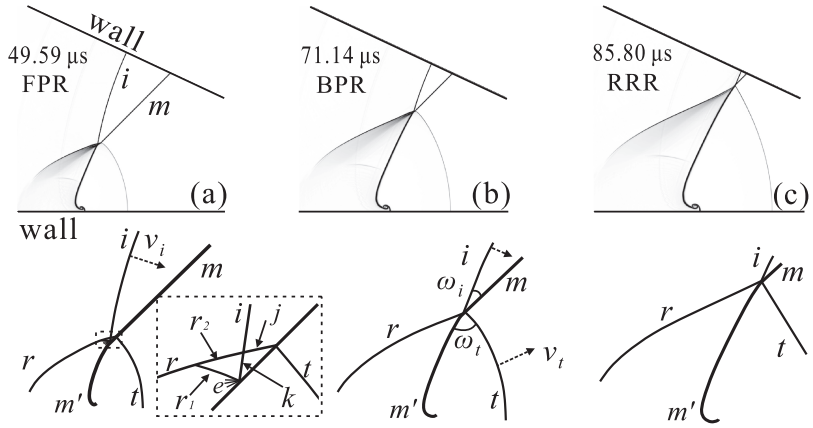

FIG. 4. Schematics of the wave patterns of a cylindrical converging shock wave refracting at a tilted interface with an initial incident angle of 45°. m', disturbed material interface; r, reflected shock; r_1, first reflected shock; r_2, second reflected shock; ω_i, incident angle; ω_t, angle of transmitted shock with gaseous interface; v_i, velocity of incident shock; v_t, velocity of transmitted shock; e, expansion waves. Other symbols are the same as those indicated in Fig. 3.

modify each other. The modified incident shock (named shock k) undergoes a regular reflection at the interface. This type of refraction at a slow/fast interface is known as free precursor refraction (FPR) which was originally observed at an air/CH_4 interface by Jahn[12] in experiment. As the shock moves inward, the incident shock intensity increases and the incident angle decreases, which will cause the transition between different wave patterns. It is shown at t = 71.14 μs that the incident shock i has caught up with the transmitted shock t along the interface. At this time, the transmitted shock t is still leaning forward, and, therefore, this type of refraction is known as bound precursor refraction (BPR), as shown in Fig. 4(b).

The displacements of some typical points on the transmitted shock (point A along the sidewall; point B at the center and point C along the interface) and on the incident shock (point D along the interface) are measured and presented in Fig. 5, together with the schematics of these points. It is found that at an early stage, the motion of the transmitted shock t is self-similar, which is analogous to the case of a planar shock refracting at an inclined interface. Therefore, the transmitted shock velocity (v_t) and the angle of the transmitted shock with the interface (ω_t) can be considered as constants at an early stage. As the shock wave converges, however, the incident shock velocity (v_i) increases and the incident angle (ω_i) decreases. Therefore, the velocity of the incident shock wave moving along the interface ($v_i/\sin\omega_i$) will increase and reach the velocity of the transmitted shock wave moving along the interface ($v_t/\sin\omega_t$), as shown in Fig. 5(b). Once the velocities of the incident and transmitted shock waves moving along the interface reach a balance, the wave pattern transition will occur (FPR → BPR here). Zeng and Takayama[18] also believed in their work that the reason for the transition of refraction configuration from BPR to FPR is that the velocity of transmitted shock wave propagating in the fast gas is larger than the velocity of the incident shock wave propagating along the interface. Besides, we should note from Fig. 5(a) that the velocities of three typical points on the transmitted shock wave coincide well at early times and disperse at late times. Especially, the velocity of the transmitted shock wave near the interface is the largest, which is different from the case of a planar shock wave refracting at an inclined interface[16,40] in which the transmitted shock wave near the interface is proven to be an evanescent wave with the strength decaying. In the present work, as the shock converges, the incident shock wave catches up with the transmitted shock wave along the interface. In the following evolution, the transmitted shock wave t owns the same velocity as the incident shock wave i along the interface. In order to better accentuate the non-self-similar nature of this flow, as shown in Fig. 6, the self-similar slope is subtracted from the original data in Fig. 5(a). Note that the self-similar slope is obtained under quasi-steady condition of a planar shock wave refracting at a planar interface, in which the planar shock wave intensity is considered as the initial converging shock intensity. One can easily find from Fig. 6 that due to the converging effect, the transmitted shock velocity becomes larger as it approaches the interface. Owing to the non-uniformity of the transmitted shock velocity, the curvature of the transmitted shock t will gradually decrease, and the

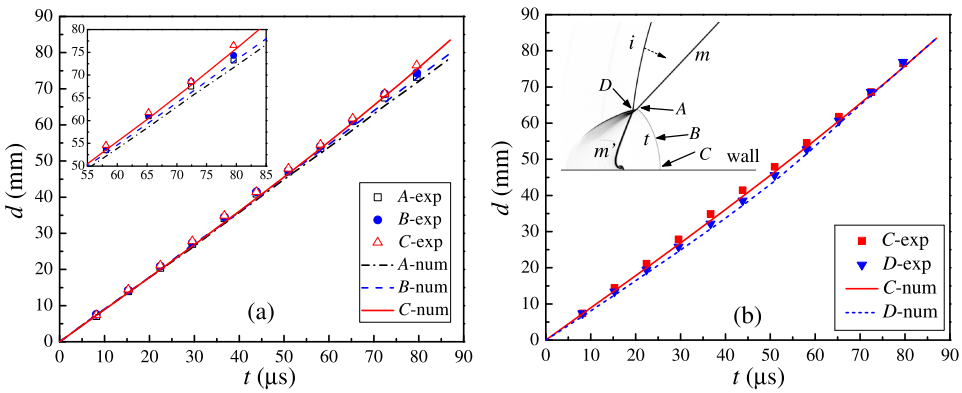

FIG. 5. Comparison of the displacements (d) of some typical points on the transmitted and incident shocks for initial incident angle ω_i = 45°.

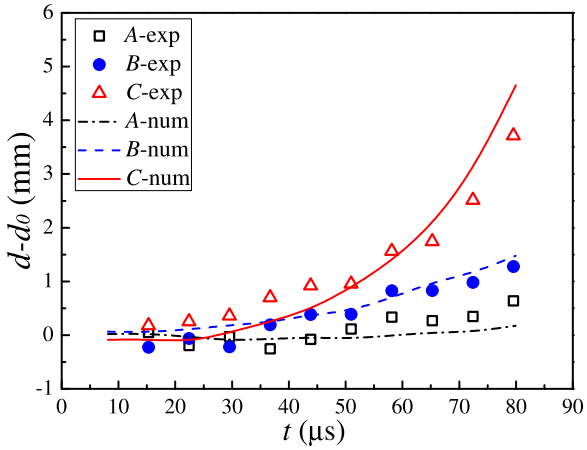

FIG. 6. Comparison of relative displacements $(d - d_0)$ of some typical points on the transmitted shock wave for initial incident angle $\omega_i = 45°$. d_0 is the displacement under quasi-steady condition of a planar shock refracting at a planar interface.

wave pattern will resemble regular refraction with reflected shock (RRR), as shown in Fig. 4(c). The BPR system differs from the RRR system both by the appearance of a fourth wave and by the fact that transmitted shock t leans forward at the interface for BPR, namely, the angle between t and the interface $\omega_t > 90°$, whereas it leans backwards for RRR ($\omega_t < 90°$).[16] Unfortunately, this phenomenon is not observed in the present experiment due to the limitation of the converging section length.

Figure 7 illustrates the experimental and numerical results of a cylindrical converging shock wave refracting at an air/helium interface with an initial incident angle $\omega_i = 60°$. Similarly, good agreement between the experimental and numerical results is reached. At an early stage, the transmitted shock wave t also moves as a free precursor shock and refracts another shock wave j into air ($t = 36.49$ μs). As depicted by the zoomed image in Fig. 8(a), the shock wave j does not interact with the incident shock wave i directly but intersects with a shock wave n. The modified shock wave n (named shock wave n') is reflected as centred expansion waves at the interface. This type of refraction at a slow/fast interface is known as twin von Neumann refraction (TNR)[15] which is characterized by two triple points tp_1 and tp_2 and a pair of von Neumann reflections. As the incident shock wave moves inward, these two triple points tp_2 and tp_1 meet each other and combine into a quadruple point (qp), as indicated at $t = 65.21$ μs in Fig. 8(b). At this moment, the shock wave n disappears and only shock wave n' remains. This type of refraction is named as twin regular refraction (TRR)[16] for it is characterized by a pair of regular reflection. Although the TRR system exists for a range of shock intensity and not just for a particular value,[16] it has never been observed in previous experiments[12,13,15] till Henderson *et al.* found it in their numerical and experimental work.[16] In the following evolution, the shock wave j detaches from the quadruple point and interacts with the incident shock wave i directly, as shown at $t = 103.47$ μs in Fig. 8(c). The modified incident shock wave (named shock wave k) undergoes a von Neumann reflection at the interface, and this type of refraction

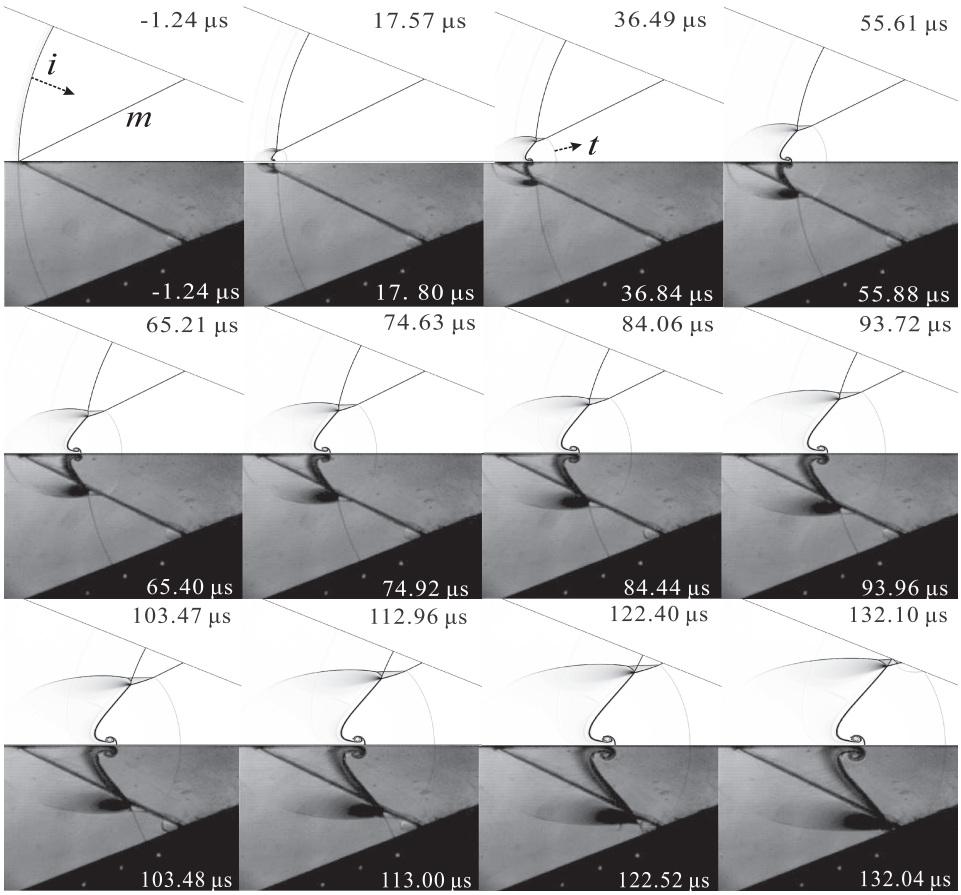

FIG. 7. Sequence of experimental and numerical schlieren frames showing the evolution of a converging shock wave refracting at a tilted interface with an initial incident angle $\omega_i = 60°$. The symbols have the same meaning as those indicated in Fig. 3.

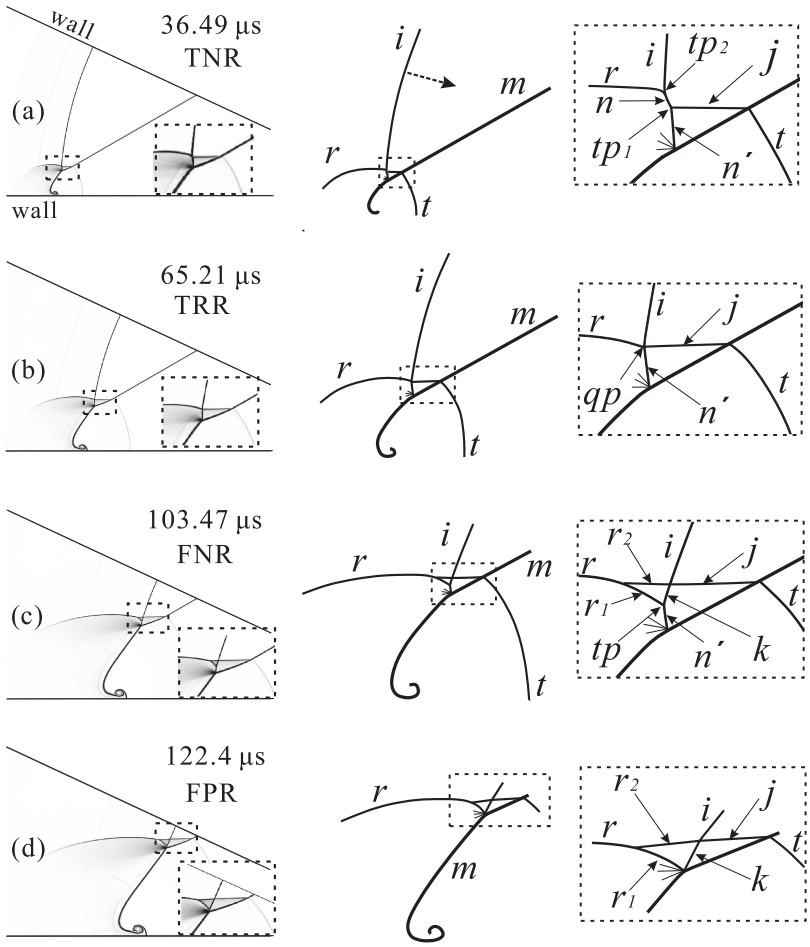

FIG. 8. Schematics of the wave patterns of a cylindrical converging shock wave refracting at a tilted interface with an initial incident angle of 45°. tp_1, the first triple point; tp_2, the second triple point; qp, the quadruple point. Other symbols are the same as those indicated in Fig. 4.

is termed as free precursor von Neumann refraction (FNR).[15] With further decrease of the incident angle, the shock wave n' is shrinking and finally disappears when it encounters the interface. As a result, as indicated in Fig. 8(d), the FNR system converts into anther irregular refraction of FPR. The difference between the FPR and FNR systems lies in that in FNR the shock wave k undergoes a von Neumann reflection at the interface while in FPR the shock wave k propagates essentially undisturbed to the interface. In the numerical simulations of a weak planar shock wave refracting at a tilted CO_2/CH_4 interface, Henderson *et al.*[16] found that with the increase of incident angle, both the wave patterns of FPR and FNR occurred in sequence. However, in previous experimental results,[15] only the transition of BPR → FNR in very weak group and the transition of BPR → FPR in weak group were observed. The transition of FPR ↔ FNR has never been found although the authors believed these two systems can convert into each other. The present result provides an experimental evidence for the wave transition from FNR to FPR for the first time.

From Fig. 8, one can conclude that the FNR system would convert into the FPR system if the shock wave k were to grow and the shock wave n' were to shrink until the shock wave k joined the interface. On the other hand, if the shock wave n' were to grow and the shock wave k were to shrink until shock wave n' joined the incident shock wave i and if the two reflected shock waves $r_{1,2}$ were to coalesce into the single shock wave r at the juncture, the FNR system would convert into the TRR system. Whether the shock wave k grows or shrinks is dependent on the velocities of the transmitted shock wave and the incident shock wave propagating along the interface. If the transmitted shock wave moves faster, the shock wave k grows, while if the transmitted shock wave moves slower, the shock wave k shrinks. This work also shows that various irregular patterns are related to each other in a continuous sequence, rather than exhibit any abrupt changes in detail, verifying the viewpoint proposed by Jahn.[12] Moreover, in previous experimental work,[15] if the incident shock intensity was held constant, the refraction pattern sequences at a slow/fast gaseous interface with increasing incident angle for very weak shock group was RRE (regular refraction with reflected expansion) →RRR → BPR → FNR, and for weak shock group was RRE → RRR → BPR → FPR → TNR → LSR (Lambda shock refraction). Later, through the numerical simulations,[16] the sequence was expanded to RRE → RRR → BPR → FPR → FNR for very weak shock group and RRE → RRR → BPR → FNR → TRR → TNR → LSR for weak shock group. In the present work, for the case of $\omega_i = 60°$, the wave patterns of TNR, TRR, FNR, and FPR occur in sequence, and the transition sequences do not belong to any groups defined by Abd-El Fattah and Henderson[15] and Henderson *et al.*[16] due to the variation of shock intensity. As a result,

the classification of the refraction phenomenon in planar case is not exhaustive or cannot be applied to the converging case.

Similarly, the displacements of some typical points on the transmitted shock wave (point E along the sidewall; point F at the center and point G along the interface) and on the incident shock wave (point H along the interface) are measured and presented in Fig. 9, together with the schematics of these points. It can be found that in this case the velocity of the transmitted shock far away from the interface is larger than the one near the interface, which is similar to the previous work,[16,40] but differs from the case of $\omega_i = 45°$. Note that during the time studied, irregular refraction always occurs and the transmitted shock wave t always moves as a free-precursor shock. Furthermore, from the schlieren images, we can observe that the distance between the points of the transmitted shock wave t and the incident shock wave i intersecting with the interface gradually increases, which illustrates that the velocity of the transmitted shock wave is larger than that of the incident shock wave along the interface although the transmitted shock wave near the interface is an evanescent wave and the incident shock velocity is increasing. Besides, because the motion of the transmitted shock wave is nearly self-similar, the angle of the shock wave j with the interface is nearly kept constant. Based on these two facts, as the incident shock wave converges, the first triple point tp_1 of the shock wave j intersecting with the shock wave n' gradually moves upward and departs away from the interface. Once the tp_1 meets the tp_2, the transition of TNR → TRR will occur. As the incident shock wave further moves inward, the shock wave j continues to move upward, modifying the incident shock wave and generating the shock wave k. The TRR system is converted into the FNR system. Further, the shock wave k is growing with the shock wave n' shrinking, and the FPR system occurs once the shock wave n' disappears. If the converging section is long enough, the BPR and RRR systems are expected to be observed later. From the discussion above, we may conclude that the transitions among different wave patterns are caused by the difference between the incident and transmitted shock waves propagating along the interface, which is determined by the incident shock strength, the incident angle, and the acoustic impedance.

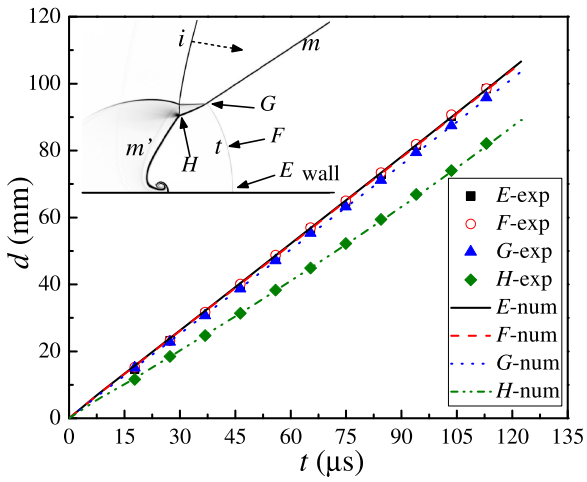

FIG. 9. Comparison of displacements of some typical points on the incident and transmitted shocks for initial incident angle $\omega_i = 60°$.

IV. CONCLUSIONS

The refraction of a cylindrical converging shock wave at an inclined air/helium interface is investigated in this work. Experimentally, a cylindrical converging shock tube is specially designed based on the shock dynamics theory to generate a perfectly cylindrical shock wave, and a soap film technique is developed to form a discontinuous inclined interface separating helium from air. The evolution of wave patterns is captured by the high-speed schlieren photography. Numerically, an upwind space-time CE/SE method is adopted to simulate the process of a cylindrical converging shock refracting at an air/helium interface. Good agreement between the experimental and numerical results implies that it is feasible to investigate the cylindrical converging shock wave refracting at an inclined gaseous interface.

The results show that during the shock wave converging process, due to the increase of incident shock velocity and decrease of incident angle, the wave patterns will transit from one to another. If the irregular refraction first occurs, the transmitted shock wave, as a free-precursor shock, will move ahead of the incident shock wave along the interface. However, the incident shock wave along the interface will speed up, causing the possible wave transition. If the initial incident angle is small, the velocity of the incident shock wave moving along the interface ($v_i/\sin\omega_i$) may be larger than that of the transmitted shock wave moving along the interface. Thus, the irregular refraction may transit into regular refraction. If the initial incident angle is large enough, the velocity of the incident shock wave may always be smaller than that of the transmitted shock wave propagating along the interface, and irregular refractions always occur. For the current study, when $\omega_i = 45°$, the results indicate that the incident shock wave eventually catches up with the transmitted shock wave, and the transitions of FPR → BPR → RRR are observed. When ω_i increases to 60°, the results indicate that the incident shock wave always falls behind the transmitted shock wave along the interface, and the transitions of TNR → TRR → FNR → FPR are observed. The transition sequences do not belong to any groups described in the planar shock case, demonstrating that the classification of the refraction phenomenon in the planar shock case is not exhaustive, or cannot be applied to the converging case. Also, it is the first time to observe the FNR → FPR transition in the experiment, providing an experimental evidence for previous numerical results. It is believed that the difference between the velocities of the incident and transmitted shock waves propagating along the interface causes the wave pattern transition.

There is clearly more to be done to advance the field of cylindrical shock refraction at an interface. In future work, the experimental image of high quality is desirable to explore the details of the wave patterns. Also the effects of incident shock strength, incident angle, and acoustic impedance on the wave pattern will be discussed thoroughly. Besides, the mechanism and criterion of the wave pattern transition need to be further investigated. In our laboratory, a new converging shock tube

with a larger cross-sectional area and a stronger shock wave is under construction, and we expect that the new facility will provide conveniences to investigate the cylindrical converging shock refraction phenomenon, and further the RM instability of an inclined interface accelerated by cylindrical converging shock waves.

ACKNOWLEDGMENTS

The authors would like to thank Dr. Hua Shen for his help on the numerical simulations. This work was supported by the National Natural Science Foundation of China (Grant Nos. 11302219, 11621202, and NSAF U1530103) and Science Challenge Project (JCKY2016212A501).

[1] J. Yang, T. Kubota, and E. E. Zukoski, "Application of shock-induced mixing to supersonic combustion," AIAA J. **31**, 854–862 (1993).
[2] J. D. Lindl, O. Landen, J. Edwards, E. Moses, and Team NIC, "Review of the national ignition campaign 2009-2012," Phys. Plasmas **21**, 020501 (2014).
[3] R. D. Richtmyer, "Taylor instability in shock acceleration of compressible fluids," Commun. Pure Appl. Math. **13**, 297–319 (1960).
[4] E. E. Meshkov, "Instability of the interface of two gases accelerated by a shock wave," Fluid Dyn. **4**, 101–104 (1969).
[5] A. H. Taub, "Refraction of plane shock waves," Phys. Rev. **72**, 51–60 (1947).
[6] H. Polachek and R. J. Seeger, "On shock-wave phenomena refraction of shock waves at a gaseous interface," Phys. Rev. **84**, 922–929 (1951).
[7] L. F. Henderson, "The refraction of a plane shock wave at a gas interface," J. Fluid Mech. **26**, 607–637 (1966).
[8] L. F. Henderson, "On shock impedance," J. Fluid Mech. **40**, 719–735 (1970).
[9] L. F. Henderson, "On the refraction of shock waves," J. Fluid Mech. **198**, 365–386 (1989).
[10] C. J. Catherasoo and B. Sturtevant, "Shock dynamics in non-uniform media," J. Fluid Mech. **127**, 539–561 (1983).
[11] D. W. Schwendeman, "Numerical shock propagation non-uniform media," J. Fluid Mech. **188**, 383–410 (1988).
[12] R. G. Jahn, "The refraction of shock waves at a gaseous interface," J. Fluid Mech. **1**, 457–489 (1956).
[13] A. M. Abd-El Fattah, L. F. Henderson, and A. Lozzi, "Precursor shock waves at a slow—Fast gas interface," J. Fluid Mech. **76**, 157–176 (1976).
[14] A. M. Abd-El Fattah and L. F. Henderson, "Shock waves at a fast-slow gas interface," J. Fluid Mech. **86**, 15–32 (1978).
[15] A. M. Abd-El Fattah and L. F. Henderson, "Shock waves at a slow-fast gas interface," J. Fluid Mech. **89**, 79–95 (1978).
[16] L. F. Henderson, P. Colella, and E. G. Puckett, "On the refraction of shock waves at a slow-fast gas interface," J. Fluid Mech. **224**, 1–27 (1991).
[17] R. R. Nourgaliev, S. Y. Sushchikh, T. N. Dinh, and T. G. Theofanous, "Shock wave refraction patterns at interfaces," Int. J. Multiphase Flow **31**, 969–995 (2005).
[18] S. M. Zeng and K. Takayama, "On the refraction of shock wave over a slow-fast gas interface," Acta Astronaut. **38**, 829–838 (1996).
[19] R. Samtaney, J. Ray, and N. Zabusky, "Baroclinic circulation generation on shock accelerated slow/fast gas interfaces," Phys. Fluids **10**, 1217–1230 (1998).
[20] J. F. Haas and B. Sturtevant, "Interaction of weak shock waves with cylindrical and spherical gas inhomogeneities," J. Fluid Mech. **181**, 41–76 (1987).
[21] R. Samtaney and N. J. Zabusky, "Circulation deposition on shock-accelerated planar and curved density-stratified interfaces: Models and scalling laws," J. Fluid Mech. **269**, 45–78 (1994).
[22] Z. Zhai, T. Si, X. Luo, and J. Yang, "On the evolution of spherical gas interfaces accelerated by a planar shock wave," Phys. Fluids **23**, 084104 (2011).
[23] R. W. Perry and A. Kantrowitz, "The production and stability of converging shock waves," J. Appl. Phys. **22**, 878–886 (1951).
[24] K. Takayama, H. Kleine, and H. Gronig, "An experimental investigation of the stability of converging cylindrical shock waves in air," Exp. Fluids **5**, 315–322 (1987).
[25] P. Dimotakis and R. Samtaney, "Planar shock cylindrical focusing by a perfect-gas lens," Phys. Fluids **18**, 031705 (2006).
[26] Z. Zhai, C. Liu, F. Qin, J. Yang, and X. Luo, "Generation of cylindrical converging shock waves based on shock dynamics theory," Phys. Fluids **22**, 041701 (2010).
[27] S. M. Bakhrakh, B. A. Klopov, E. E. Meshkov, A. I. Tolshmyakov, and Y. V. Yanilkin, "Development of perturbations of a shock-accelerated interface between two gases," J. Appl. Mech. Tech. Phys. **36**, 341–346 (1995).
[28] T. Wang, J. H. Liu, J. S. Bai, Y. Jiang, P. Li, and K. Liu, "Experimental and numerical investigation of inclined air/SF_6 interface instability under shock wave," Appl. Math. Mech. **33**, 37–50 (2012).
[29] J. A. McFarland, D. Reilly, S. Creel, C. McDonald, T. Finn, and D. Ranjan, "Experimental investigation of the inclined interface Richtmyer-Meshkov instability before and after reshock," Exp. Fluids **55**, 1640–1653 (2014).
[30] J. A. McFarland, D. Reilly, W. Black, J. A. Greenough, and D. Ranjan, "Modal interactions between a large-wavelength inclined interface and small-wavelength multimode perturbations in a Richtmyer-Meshkov instability," Phys. Rev. E **92**, 013023 (2015).
[31] D. Reilly, J. A. McFarland, M. Mohaghar, and D. Ranjan, "The effects of initial conditions and circulation deposition on the inclined-interface reshocked Richtmyer-Meshkov instability," Exp. Fluids **56**, 168–183 (2015).
[32] X. Luo, P. Dong, T. Si, and Z. Zhai, "The Richtmyer-Meshkov instability of a 'V' shaped air/SF_6 interface," J. Fluid Mech. **802**, 186–202 (2016).
[33] Z. Zhai, P. Dong, T. Si, and X. Luo, "The Richtmyer-Meshkov instability of a 'V' shaped air/helium interface subjected to a weak shock," Phys. Fluids **28**, 082104 (2016).
[34] X. Luo, T. Si, J. Yang, and Z. Zhai, "A cylindrical converging shock tube for shock-interface studies," Rev. Sci. Instrum. **85**, 015107 (2014).
[35] S. H. R. Hosseini and K. Takayama, "Experimental study of Richtmyer-Meshkov instability induced by cylindrical shock waves," Phys. Fluids **17**, 084101 (2005).
[36] M. Wang, T. Si, and X. Luo, "Generation of polygonal gas interfaces by soap film for Richtmyer-Meshkov instability study," Exp. Fluids **54**, 1427–1435 (2013).
[37] H. Shen, C. Y. Wen, and D. L. Zhang, "A characteristic space-time conservation element and solution element method for conservation laws," J. Comput. Phys. **288**, 101–118 (2015).
[38] H. Shen and C. Y. Wen, "A characteristic space-time conservation element and solution element method for conservation laws. II. Multidimensional extension," J. Comput. Phys. **305**, 775–792 (2016).
[39] H. Shen, C. Y. Wen, K. X. Liu, and D. L. Zhang, "Robust high-order space-time conservative schemes for solving conservation laws on hybrid meshes," J. Comput. Phys. **281**, 375–402 (2015).
[40] Z. Zhai, M. Wang, T. Si, and X. Luo, "On the interaction of a planar shock with a light polygonal interface," J. Fluid Mech. **757**, 800–816 (2014).